ACCELERATOR BEAMLINE PERFORMANCE FOR THE IR FEL AT THE FRITZ-HABER-INSTITUT, BERLIN

H. P. Bluem#, D. Dowell*, H. Loos*, J. Park, A. M. M. Todd and L. M. Young*
Advanced Energy Systems, Medford, NY, USA.
S. Gewinner and W. Schöllkopf
Fritz-Haber-Institut der Max-Planck-Gesellschaft, Berlin, Germany.

Abstract

An electron accelerator and beamline for an IR and THz FEL with a design wavelength range from 4 to 500 µm has been commissioned by Advanced Energy Systems at the Fritz-Haber-Institut (FHI) [1] in Berlin, Germany, for applications in molecular and cluster spectroscopy as well as surface science. The linac comprises two S-band standing-wave copper structures and was designed to meet challenging specifications, including a final energy adjustable in the range of 15 to 50 MeV, low longitudinal emittance (< 50 keV-psec) and transverse emittance (< 20 π mm-mrad), at more than 200 pC bunch charge with a micro pulse repetition rate of 1 GHz. First lasing was achieved February 2012.

INTRODUCTION

The FHI FEL shown in Figure 1 will be utilized for research in gas-phase spectroscopy of (bio-)molecules, clusters, and nano-particles, as well as in surface science. Advanced Energy Systems (AES) has designed and installed the accelerator and electron beam transport system. STI Optronics fabricated the 40 mm-period MIR undulator [2] with Bestec GmbH delivering the MIR oscillator mirror optical equipment [3]. The FIR beamline has not yet been installed. We describe the achievement of first light at 16 microns and present the performance milestones achieved.

SYSTEM DESCRIPTION

The design, fabrication and installation of the FEL has been described previously [4,5,6]. The accelerator system is comprised of a gridded gun followed by a 1 GHz sub-harmonic buncher and two 3 GHz, pi/2 copper linac structures. A chicane between the linacs affords bunch length control of the 20 MeV beam out of linac-1. Linac-2 can then be operated in accel or decel mode to provide beams at 15 to 50 MeV to isochronous bends directing beam to the undulators or to a diagnostic station.

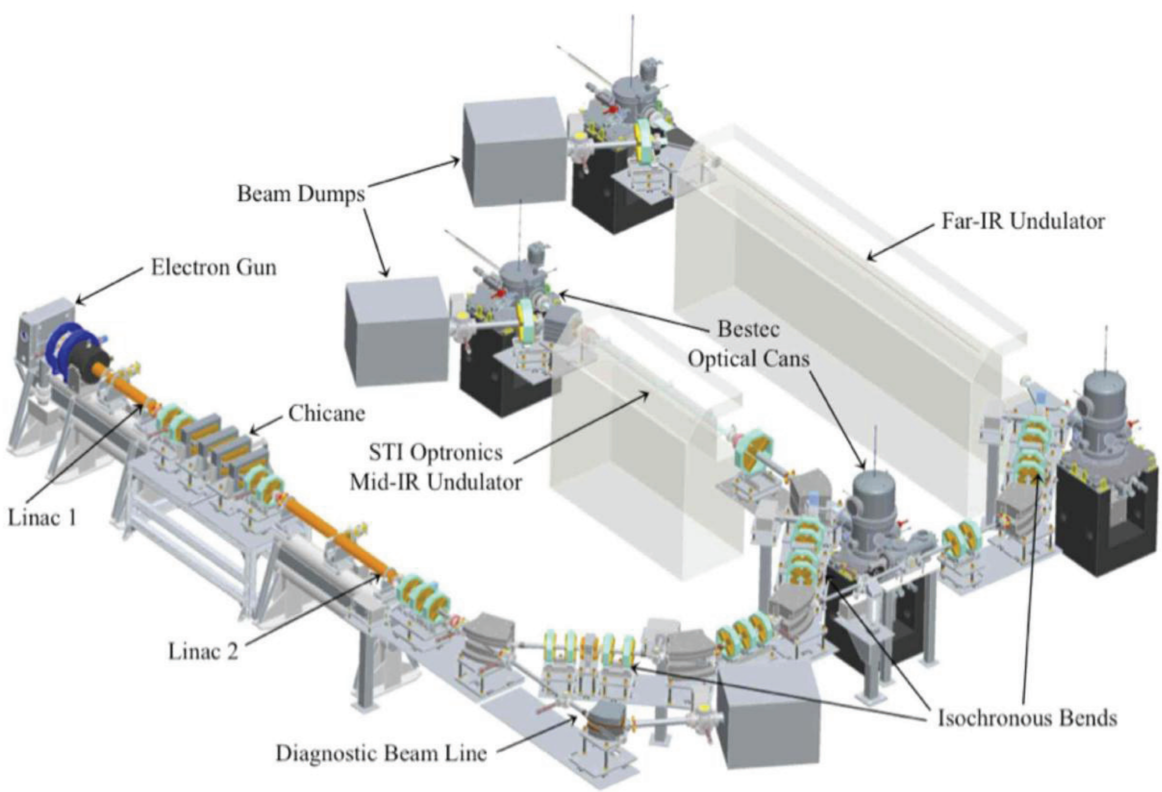

Figure 1: Schematic diagram of the Fritz Haber Institute FEL showing key components.

hans_bluem@mail.aesys.net
* Consultants to AES

ISBN 978-3-95450-123-6

Figure 2: The MIR FEL installation in the FHI vault.

The Figure 2 photograph shows the MIR FEL installation in the FHI vault from roughly the same perspective as Figure 1. The gun and chicane, which are not particularly clear in Figure 2, but are critical components of the system, are shown separately in Figures 3 and 4.

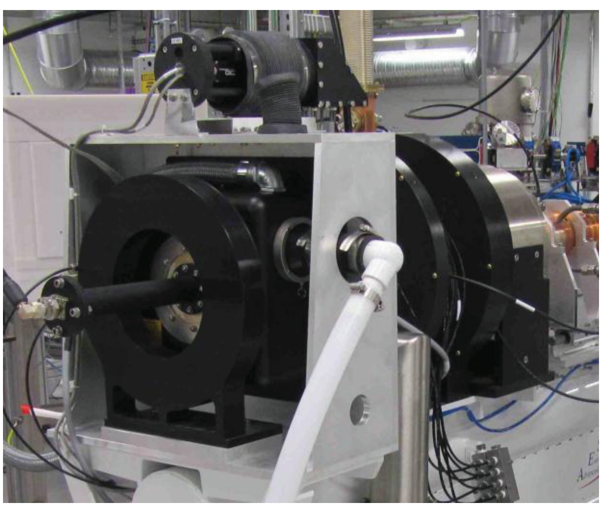

Figure 3: Gridded thermionic gun of the MIR FEL.

Figure 4: FEL chicane between quadrupole doublets.

FEL COMMISSIONING AND FIRST LIGHT

RF conditioning of the accelerating structures began in late August of 2011. First gun operation took place in mid September. By the middle of October, we had succeeded in delivering a 35 pC beam to the MIR beam dump. Through the remainder of 2011, we made improvements to the low level RF (LLRF) system, increased the delivered RF power to the accelerators, increased the gun current and worked on the energy spread and bunch length.

At the start of 2012, we began to work towards lasing in earnest. A number of issues in the RF system slowed commissioning, including loss of tuning in the master source, a large phase jitter present in the subharmonic buncher drive and issues affecting one of the klystrons. Despite the phase jitter in the subharmonic buncher, an arrangement of phase settings could be found that resulted in an electron beam energy that was relatively insensitive to the subharmonic buncher phase. This was key to achieving first lasing.

Once energy stability was achieved, the beam was sent through the wiggler resulting in the observation of spontaneous emission in Figure 5. In the figure, the yellow trace represents 200 mA at the exit of the second linac. The red and green traces are the signals from current transformers at the entrance and exit of the wiggler. These traces indicate that the initial 3 μs of the beam pulse had a significant spread in energy so some of the electrons were lost through the isochronous bends. However, the final 2 μs shows near 100% transmission of the beam through the wiggler. The white trace is the baseline mercury cadmium telluride (MCT) signal with no beam, while the blue trace shows the energy from the spontaneous emission.

ISBN 978-3-95450-123-6

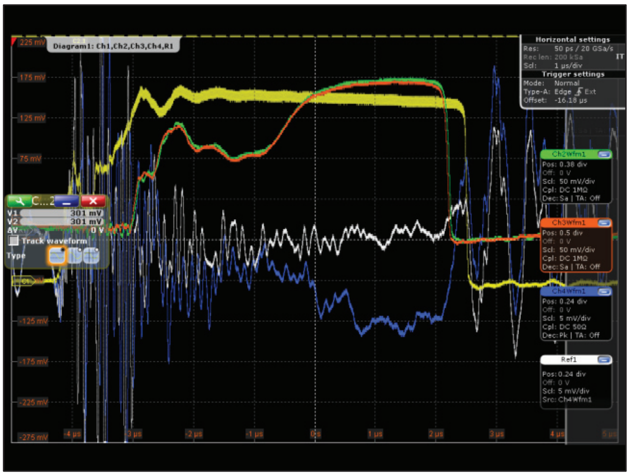

Figure 5: Observation of spontaneous emission with a mercury cadmium telluride (MCT) detector – blue trace.

The following day, at 28 MeV, after aligning the electron beam in the wiggler, with a wiggler gap of 20 mm corresponding to a wiggler parameter K_{rms} = 1.22, we achieved first light at 16 microns. This is shown in Figure 6. The saturated MCT detector trace is blue, the current transformer signal indicating > 200 mA (corresponding to 210 pC) is red, while the green and yellow traces are the subharmonic buncher phase and amplitude. The issues with the subharmonic buncher phase can be seen in the green curve of Figure 6, which, in addition to a large slew, also has a substantial thickness, indicating the shot-to-shot variation that was present prior to modification. More details on the MIR FEL oscillator can be found in Ref. [3].

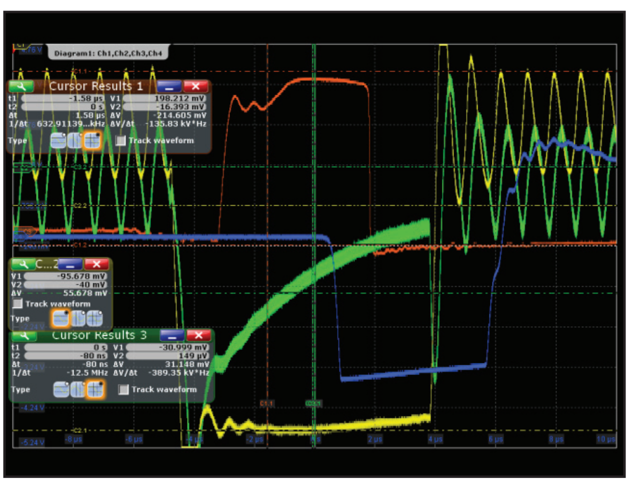

Figure 6: Saturated MCT detector signal in blue confirming first light.

ACCELERATOR PERFORMANCE MEASUREMENTS

The electron beam performance we are seeking to achieve is given in Table 1. Where a specification value is shown in parentheses, this is a target upgrade parameter and not the base performance of the system. Table 1 also shows the measured performance that has been achieved to date.

Table 1: FHI FEL Electron Beam Parameters

Parameter	Unit	Specification	Achieved
Electron Energy	MeV	(15) 20 - 50	20 - 50
Energy Spread	%	(<) 0.1	0.1
Energy Drift per Hour	%	(<) 0.1	TBD
Bunch Charge	pC	(>) 200	215
Micropulse Length	psec	1 - 5 (10)	2.5
Micropulse Repetition Rate	GHz	1	1
Micropulse Jitter	psec	0.5 (0.1)	TBD
Macropulse Length	µsec	1 - 8 (15)	1 - 8
Macropulse Repetition Rate	Hz	10 (20)	1
Transverse RMS Emittance	π mm-mrad	20	15.3

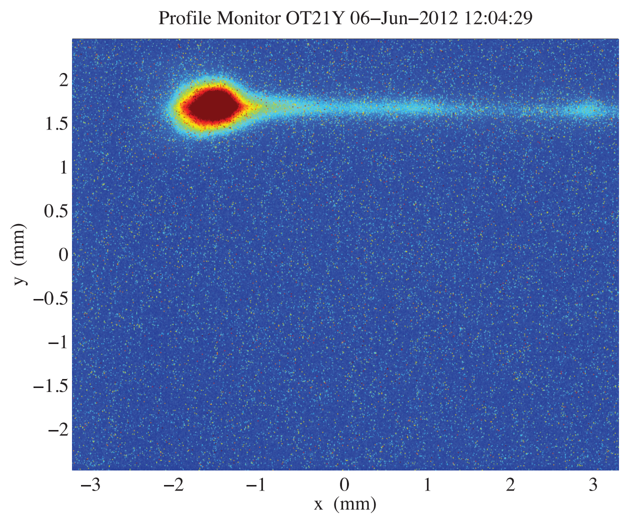

Figure 7: Electron beam image from energy measurement YAG screen in diagnostic beamline.

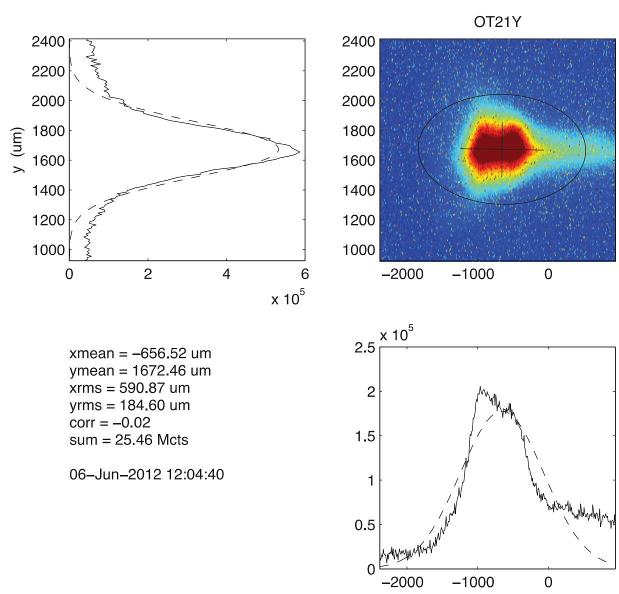

Figure 8: Beam size measurement for the image in Figure 7 representing ~ 0.1% energy spread at 45 MeV.

The dispersed electron beam on the diagnostic energy screen is shown in Figure 7. The corresponding profile measurement is depicted in Figure 8. The gaussian fitted horizontal size of 590 µm rms represents an energy spread

ISBN 978-3-95450-123-6

slightly above 0.1%. The saturation of the video clearly needs to be reduced in order to achieve a more accurate measurement. Previous measurements indicated an energy spread below 0.1%. We also performed some initial measurements to estimate the length of the micropulses. This was accomplished by measuring the energy spread with the second linac structure set to zero energy gain (i.e. balancing the beamloading with minimal RF power), then setting the field amplitude to a known level with the phase 90° from the microbunch phase and remeasuring the energy spread. With the chicane on and off, the bunch length was estimated to be 2 psec and 5 psec respectively.

The results of a quadrupole scan are shown in Figure 9. A horizontal emittance of 15.3 π mm-mrad was measured for a 45 MeV, 125 mA beam. The ± 3% statistical error is quite good and comes from the random variation in the measurements, mostly reflecting shot-to-shot stability.

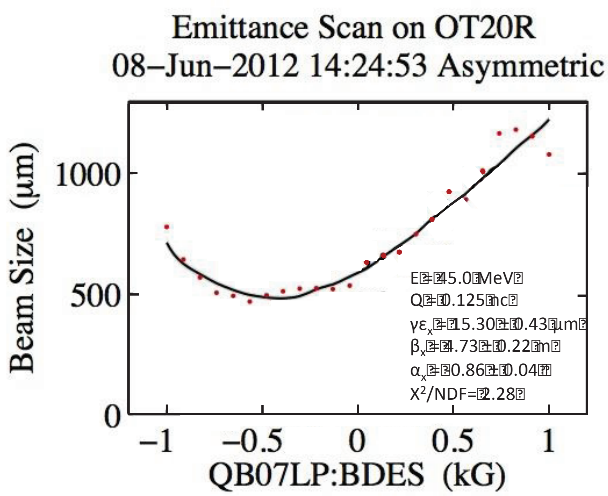

Figure 9: Emittance scan for 125 mA, 45 MeV beam.

We have achieved the base energy range but have not yet operated the second accelerator in a decelerating mode to deliver beam energies lower than 20 MeV. The energy spread requirement has been met at 25 MeV and at 45 MeV. Currents in excess of the specified 200 pC have already been achieved at the 1 GHz micropulse repetition rate. The transverse emittance measurements indicate the beam quality is at least very close to the expected level, but still needs to be verified at full current once issues with the gun high voltage power supply are resolved. The preliminary bunch length measurements are also very encouraging. The 1 Hz RF macropulse pulse repetition rate is temporary and not intrinsic to the system.

Since first light, we have successfully implemented a LLRF feedforward system that will greatly aid in the upcoming acceptance testing. The feedforward system is designed to help compensate for the cavity filling transients. The fields are sampled with the demodulated I&Q signals and then fed into an ADC for the controls to read and operate on. The same system is used to provide a slow feedback to reduce the long term drift of the beam energy. The subharmonic buncher provides an added challenge since the electron beam induced signal dominates the RF drive. The upper trace of Figure 10 shows the subharmonic buncher Q signal prior to the feedforward being applied. Two features of note are the overshoot transient at the beginning of the pulse and the step down to a lower level when the electron beam shuts down. After feedforward is applied, the new modified signal achieved is the Figure 10 lower trace. The fill time transient is greatly reduced as is the beam turn-off transient. The lower level at the end of the pulse is used for the slow feedback of the subharmonic buncher RF drive to improve the long term stability of the amplitude and phase. Similar feedforward is applied to both of the linac RF drives.

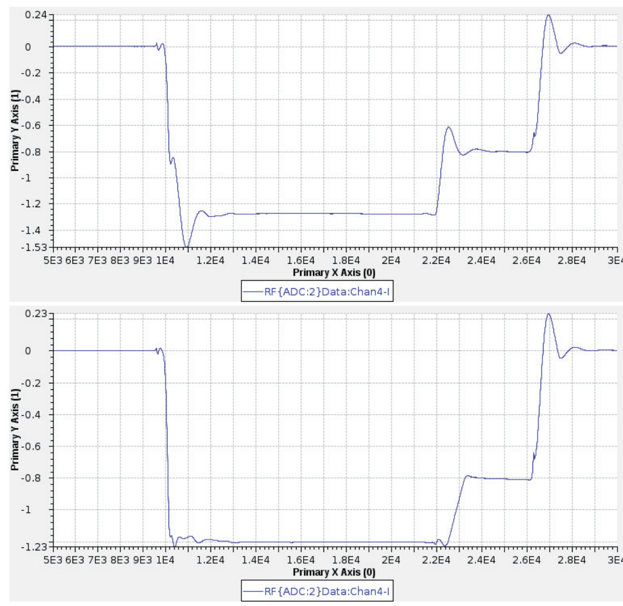

Figure 10: Subharmonic buncher Q signal without (upper) and with (lower) LLRF feed forward.

SUMMARY

The installation of the MIR beamline for the FHI FEL has been completed and commissioning is well underway. A number of equipment issues have been identified and most have been resolved. Beam was first delivered to the MIR beam dump in mid October 2011 just before the FHI Centennial. First light at ~ 16 microns was achieved on February 14, 2012. We are now in the final push towards mid-IR acceptance.

REFERENCES

[1] http://www.fhi-berlin.mpg.de/mp/

[2] Gottschalk, et al., these proceedings, Paper THPD13.

[3] Schöllkopf et al., these proceedings, Paper MOOB1.

[4] H. Bluem et al., “The Fritz Haber Institute THz FEL Status”, http://accelconf.web.cern.ch/accelconf /FEL2010/papers/mopa09.pdf

[5] W. Schöllkopf et al., “Status of the Fritz Haber Institute THz FEL”, http://accelconf.web.cern.ch /accelconf/FEL2011/papers/tupb30.pdf

[6] A. M. M. Todd et al., “Commissioning Status of the Fritz Haber Institute THz FEL”, http://accelconf.web .cern.ch/accelconf/IPAC2011/papers/thpc106.pdf

ISBN 978-3-95450-123-6